Quantization Model for Multiresolution Dyadic Subband Tree Structure

Ginkyu Choi
Department of Electrical Engineering
Polytechnic University
5 Metrotech Center, Brooklyn, NY 11201
E-mail : gchoi@prism.poly.edu

R. A. Haddad
Department of Electrical Engineering
Polytechnic University
5 Metrotech Center, Brooklyn, NY 11201
E-mail : rhaddad@ishara.poly.edu

Abstract

In this paper, we develop a methodology for the analysis of signal quantization effects in dyadic subband tree structures using the gain-plus-additive noise model for the pdf-optimized quantizer. We constrain the non-quantized and uncompensated structure to be PR(Perfect Reconstruction). We develop an equivalent polyphase structure, and compute the MSE(Mean Square Error) using cyclostationary concepts in terms of (1) the allocated quantizer bits, (2) the filter coefficients, and (3) an embedded compensation parameter vecter $\underline{K}$. This MSE is then minimized over all three items above. Our optimization method is applied to the specific case of a four channel dyadic tree. This tree is represented by an eight channel polyphase equivalent whose interchannel signals are correlated. Our design of a 4-tap paraunitary structure is confirmed by simulation.

1 Introduction

Fig. 5 shows the composite analysis/synthesis structure for a three level (or four channel) dyadic tree. PR in the absence of quantizers is satisfied if innermost (from A to B) two band is PR and next outer two band is PR, and so on. Fig. 5 can be equivalently converted to Fig. 6 using the gain-plus-additive noise model for the pdf-optimized quantizer, and multirate equivalences. In Fig. 6, the total data rate for the subband signals at the output of the analysis section equals f_s [sample/sec], the data rate of the source signal. So it is a critically sampled dyadic tree. Note that the PR condition is no longer valid when a quantizer is inserted at each channel even though PR-satisfied filters are used. Fig. 8 is an eight channel equivalent to Fig. 6 [2]. A characteristic feature of this eight channel structure is that correlations between channels are present and must be considered carefully.

Fig. 7 shows the gain-plus-additive noise model used for each quantizer followed by a compensation parameter $\underline{K}$ whose value is to be optimized [4].

The final equivalent structure is shown in Fig. 9. The filter banks are represented by polyphase equivalent matrices, the quantizer by the gain-plus-additive noise model, and the compensation by the embedded gains $\underline{K}$.

2 Quantizer model

The gain-plus-additive noise for the pdf-optimized quantizer followed by compensator as in Fig. 7 has the following main properties [1] [3] [7];

(i) if $E\{(x-\hat{x})\}=0$ and $E\{(x-\hat{x})\hat{x}\}=0$ (quantization error is zero mean and quantization error is orthogonal to quantized output), then $E\{xr\}=0$ (input and equivalent additive noise are uncorrelated)implies

(ii) $\sigma_r^2=\alpha(1-\alpha)\sigma_x^2$

(iii) $\alpha=1-\gamma 2^{-2R}$, $\gamma=\gamma(R)$, $R=$ allocated bits.

(iv) $\mathrm{Var}\{\hat{x}\}=\alpha^2\sigma_x^2+\sigma_r^2$

3 MSE formulation

With reference to Fig. 9, we define $y'(n)$ as the output with quantizers present, and $y(n)$ as the output with zero quantization errors. For PR in absence of quantizers, $y(n)=x(n-n_0)$, where n_0 is the equivalent delay.

The MSE due to quantization in Fig. 9 is

$$\begin{aligned}\mathrm{MSE} &\triangleq \frac{1}{8}\sum_{n-7}^{n} E\{(y'(n)-y(n))^2\}\\ &= \overline{R}_{y'y'}(0)-2\overline{R}_{y'y}(0)+\overline{R}_{yy}(0)\\ &= \tfrac{1}{2\pi j}\oint\left\{\overline{S}_{y'y'}(z)-2\overline{S}_{y'y}(z)+\overline{S}_{yy}(z)\right\}z^{-1}dz \qquad (1)\end{aligned}$$

$\overline{R}_{y'y'}(k)$ is average over one period of the cyclostationary correlation, and $\overline{R}_{y'y}(k)$, $\overline{R}_{yy}(k)$ are similarly defined [5]. $\overline{S}_{y'y'}(z)$ is the PSD(Power Spectral Density), the Z transform of $\overline{R}_{y'y'}(k)$.

It has been shown that this MSE can be expressed using cyclostationary concepts [5] [6] [8] as the sum of two components, a signal distortion component σ_D^2, and σ_N^2, the component due to the additive noise in the quantizer model.

$$MSE \quad = \quad \sigma_D^2+\sigma_N^2 \qquad (2)$$

where

$$\sigma_D^2 = \frac{1}{2\pi j}\oint \frac{1}{8} D(z)\mathcal{G_P}'(z^8)\Big\{AK\mathcal{H_P}(z^8)S'_{\underline{xx}}(z)$$
$$\cdot \mathcal{H_P}^T(z^{-8})(AK - 2I_8) + \mathcal{H_P}(z^8)S'_{\underline{xx}}(z)\mathcal{H_P}^T(z^{-8})\Big\}$$
$$\cdot \mathcal{G_P}'^T(z^{-8})D^T(z^{-1})z^{-1}dz \quad (3)$$

$$\sigma_N^2 = \frac{1}{2\pi j}\oint \frac{1}{8} D(z)\mathcal{G_P}'(z^8)KS_{\underline{rr}}(z^8)K$$
$$\cdot \mathcal{G_P}'^T(z^{-8})D^T(z^{-1})z^{-1}dz \quad (4)$$

where

$$D(z) = [z^{-7}, z^{-6}, \cdots, 1], \quad A = \mathrm{diag}\{\alpha_0, \alpha_1, \cdots, \alpha_3\},$$

$$K = \mathrm{diag}\{k_0, k_1, \cdots, k_3\}.$$

$\mathcal{H_P}(z)$: dyadic polyphase matrix at analysis section
$\mathcal{G_P}'(z)$: dyadic polyphase matrix at synthesis section
$S_{\underline{rr}}(z)$: Z-transform of fictitious 8×8 noise covariance matrix [1].

$$S'_{\underline{xx}}(z) = \begin{bmatrix} S'_{xx}(0) & S'_{xx}(1) & \cdots & S'_{xx}(7) \\ S'_{xx}(-1) & S'_{xx}(0) & \cdots & S'_{xx}(6) \\ \vdots & \vdots & \ddots & \vdots \\ S'_{xx}(-7) & S'_{xx}(-6) & \cdots & S'_{xx}(0) \end{bmatrix}$$

where

$$S'_{xx}(a) \triangleq \frac{1}{8} z^a \sum_{k=0}^{7} W_8^{-ka} S_{xx}(zW_8^{-k}), \quad -7 \leq a \leq 7$$

We can set the signal distortion $\sigma_D^2 = 0$, by selecting $AK = I_8$, leaving us with

$$\sigma_N^2 = \frac{1}{2\pi j}\oint \frac{1}{8} D(z)\mathcal{G_P}'(z^8)KS_{\underline{rr}}(z^8)K$$
$$\cdot \mathcal{G_P}'^T(z^{-8})D^T(z^{-1})z^{-1}dz \quad (5)$$

But this choice is not necessarily optimal. The matrices are called dyadic polyphase matrices with special properties. For the 8×8 case considered here, each can be represented by four primitive submatrices of two 1×2, one 2×2, and one 4×2 shown by dashed line partitioning below. All other submatrices are a shuffling and delay of these primitives. The dyadic polyphase matrix, $\mathcal{H_P}(z)$, is expressed as

$$\mathcal{H_P}(z) = \begin{bmatrix} A_{00}(z) & A_{01}(z) & A_{02}(z) & A_{03}(z) & A_{04}(z) & A_{05}(z) & A_{06}(z) & A_{07}(z) \\ A_{10}(z) & A_{11}(z) & A_{12}(z) & A_{13}(z) & A_{14}(z) & A_{15}(z) & A_{16}(z) & A_{17}(z) \\ A_{20}(z) & A_{21}(z) & A_{22}(z) & A_{23}(z) & A_{24}(z) & A_{25}(z) & A_{26}(z) & A_{27}(z) \\ A_{24}(z) & A_{25}(z) & A_{26}(z) & A_{27}(z) & zA_{20}(z) & zA_{21}(z) & zA_{22}(z) & zA_{23}(z) \\ A_{30}(z) & A_{31}(z) & A_{32}(z) & A_{33}(z) & A_{34}(z) & A_{35}(z) & A_{36}(z) & A_{37}(z) \\ A_{32}(z) & A_{33}(z) & A_{34}(z) & A_{35}(z) & A_{36}(z) & A_{37}(z) & zA_{30}(z) & zA_{31}(z) \\ A_{34}(z) & A_{35}(z) & A_{36}(z) & A_{37}(z) & zA_{30}(z) & zA_{31}(z) & zA_{32}(z) & zA_{33}(z) \\ A_{36}(z) & A_{37}(z) & zA_{30}(z) & zA_{31}(z) & zA_{32}(z) & zA_{33}(z) & zA_{34}(z) & zA_{35}(z) \end{bmatrix}$$

The 2×2 primitive is

$$\begin{bmatrix} A_{20} & A_{21} \\ A_{24} & A_{25} \end{bmatrix} = \begin{bmatrix} [H''_{10}H''_{11}H''_{12}H''_{13}] \begin{bmatrix} 1 & 0 & 0 & 0 \\ 0 & 0 & 0 & z^{-1} \\ 0 & 0 & z^{-1} & 0 \\ 0 & z^{-1} & 0 & 0 \end{bmatrix} \\ [H''_{10}H''_{11}H''_{12}H''_{13}] \begin{bmatrix} 0 & 0 & 1 & 0 \\ 0 & 1 & 0 & 0 \\ 1 & 0 & 0 & 0 \\ 0 & 0 & 0 & z^{-1} \end{bmatrix} \end{bmatrix} \begin{bmatrix} H'_{00} & H'_{01} \\ H'_{02} & H'_{03} \\ H'_{04} & H'_{05} \\ H'_{06} & H'_{07} \end{bmatrix}$$

The remaining 2×2 submatrices are

$$\begin{bmatrix} A_{22} & A_{23} \\ A_{26} & A_{27} \end{bmatrix} = \begin{bmatrix} [H''_{10}H''_{11}H''_{12}H''_{13}] \begin{bmatrix} 0 & 1 & 0 & 0 \\ 1 & 0 & 0 & 0 \\ 0 & 0 & 0 & z^{-1} \\ 0 & 0 & z^{-1} & 0 \end{bmatrix} \\ [H''_{10}H''_{11}H''_{12}H''_{13}] \begin{bmatrix} 0 & 0 & 0 & 1 \\ 0 & 0 & 1 & 0 \\ 0 & 1 & 0 & 0 \\ 1 & 0 & 0 & 0 \end{bmatrix} \end{bmatrix} \begin{bmatrix} H'_{00} & H'_{01} \\ H'_{02} & H'_{03} \\ H'_{04} & H'_{05} \\ H'_{06} & H'_{07} \end{bmatrix}$$

$$\begin{bmatrix} A_{24} & A_{25} \\ zA_{20} & zA_{21} \end{bmatrix} = \begin{bmatrix} [H''_{10}H''_{11}H''_{12}H''_{13}] \begin{bmatrix} 0 & 0 & 1 & 0 \\ 0 & 1 & 0 & 0 \\ 1 & 0 & 0 & 0 \\ 0 & 0 & 0 & z^{-1} \end{bmatrix} \\ [H''_{10}H''_{11}H''_{12}H''_{13}] \begin{bmatrix} z & 0 & 0 & 0 \\ 0 & 0 & 0 & 1 \\ 0 & 0 & 1 & 0 \\ 0 & 1 & 0 & 0 \end{bmatrix} \end{bmatrix} \begin{bmatrix} H'_{00} & H'_{01} \\ H'_{02} & H'_{03} \\ H'_{04} & H'_{05} \\ H'_{06} & H'_{07} \end{bmatrix}$$

$$\begin{bmatrix} A_{26} & A_{27} \\ zA_{22} & zA_{23} \end{bmatrix} = \begin{bmatrix} [H''_{10}H''_{11}H''_{12}H''_{13}] \begin{bmatrix} 0 & 0 & 0 & 1 \\ 0 & 0 & 1 & 0 \\ 0 & 1 & 0 & 0 \\ 1 & 0 & 0 & 0 \end{bmatrix} \\ [H''_{10}H''_{11}H''_{12}H''_{13}] \begin{bmatrix} 0 & z & 0 & 0 \\ z & 0 & 0 & 0 \\ 0 & 0 & 0 & 1 \\ 0 & 0 & 1 & 0 \end{bmatrix} \end{bmatrix} \begin{bmatrix} H'_{00} & H'_{01} \\ H'_{02} & H'_{03} \\ H'_{04} & H'_{05} \\ H'_{06} & H'_{07} \end{bmatrix}$$

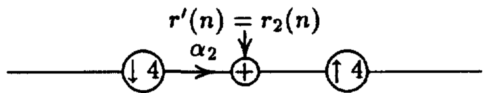

Fig.1

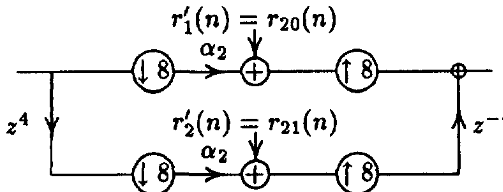

Fig.2

In order to get the second 2×2 submatrix, shift right each row of the previous 4×4 submatrices. But the element that spills over during the right shift is circulated back after multiplying with z.

The dyadic tree of Fig. 5 tries to decompose the input signal spectrum into four separate frequency band. The signals at the inputs to each quantizer are only weakly correlated. Therefore the quantization noise of the four separate bands are even less correlated. We assume uncorrelated cross band noise in Fig. 6. The 8 channel decomposition in Fig. 8 shows noise sources derived from the 4 band tree. The equivalent noise sources within each channel are defined as illustrated in Fig. 1 and Fig. 2 for noise source $r_2(n)$. It follows that

$$R_{r_1'r_1'}(k) = R_{r'r'}(2k), R_{r_1'r_2'}(k) = R_{r'r'}(2k+1)$$

$$R_{r_2'r_1'}(k) = R_{r'r'}(2k-1), R_{r_2'r_2'}(k) = R_{r'r'}(2k)$$

If $r'(n)$ is white noise, $R_{r'r'}(k) = \sigma^2_{r'}\delta(k)$, then $R_{r_1'r_2'}(k) = 0$, for all integer k. That is, the cross channel noise within the same band are uncorrelated. Now $S_{\underline{rr}}(z)$ is an 8×8 diagonal matrix.

Also we can show that the MSE for any PR structure is minimized by choosing

$$\underline{K} \;=\; 2\{A(P+P^T)A + Q + Q^T\}^{-1}AT \qquad (6)$$

where

$$P = \frac{1}{2\pi j}\oint \mathrm{diag}\left\{D(z)\mathcal{G_P}'(z^8)\right\}\mathcal{H_P}(z^8)S'_{\underline{xx}}(z) \cdot {\mathcal{H_P}}^T(z^{-8})\mathrm{diag}\left\{{\mathcal{G_P}'}^T(z^{-8})D^T(z^{-1})\right\}z^{-1}dz$$

$$Q = \frac{1}{2\pi j}\oint \mathrm{diag}\left\{D(z)\mathcal{G_P}'(z^8)\right\}S_{\underline{rr}}(z^8) \cdot \mathrm{diag}\left\{{\mathcal{G_P}'}^T(z^{-8})D^T(z^{-1})\right\}z^{-1}dz$$

$$T = \frac{1}{2\pi j}\oint \mathrm{diag}\left\{D(z)\mathcal{G_P}'(z^8)\right\}\mathcal{H_P}(z^8)S'_{\underline{xx}}(z) \cdot {\mathcal{H_P}}^T(z^{-8}){\mathcal{G_P}'}^T(z^{-8})D^T(z^{-1})z^{-1}dz$$

These results are very general; the only requirement is that each nested two channel analysis/synthesis structure be PR. We have particularized these results for the 4 tap paraunitary and the biorthogonal realization with identical nested structures ($H_0' = H_0'' = H_0'''$), and { ($H_0' = H_0'' = H_0'''$), ($H_1' = H_1'' = H_1'''$) } respectively. In this case,

$$\sigma_D^2 \;=\; \frac{1}{2\pi j}\oint \frac{1}{8}G(z)AKS'_{\underline{HH}}(z)AKG^T(z^{-1})z^{-1}dz$$
$$\frac{-1}{2\pi j}\oint \frac{1}{4}S_{xx}(z)\,z^{21}\,G(z)\,A\,K\,H^T(z)\,z^{-1}\,dz$$
$$+R_{xx}(0) \qquad (7)$$

$$\sigma_N^2 \;=\; \frac{1}{2\pi j}\oint \frac{1}{8}G(z)KS_{\underline{rr}}(z^8)KG^T(z^{-1})z^{-1}dz \qquad (8)$$

where

$$G(z) = [B_0, B_1, B_2, z^{-4}B_2, B_3, z^{-2}B_3, z^{-4}B_3, z^{-6}B_3]$$

$$H(z) = [A_0, A_1, A_2, z^4A_2, A_3, z^2A_3, z^4A_3, z^6A_3]$$

$$S'_{\underline{HH}}(z) = \begin{bmatrix} S'_{HH}(0,0) & S'_{HH}(0,1) & \cdots & S'_{HH}(0,7) \\ S'_{HH}(1,0) & S'_{HH}(1,1) & \cdots & S'_{HH}(1,7) \\ \vdots & \vdots & \ddots & \vdots \\ S'_{HH}(7,0) & S'_{HH}(7,1) & \cdots & S'_{HH}(7,7) \end{bmatrix}$$

where

$$S'_{HH}(r,c) \triangleq \frac{1}{8}\sum_{k=0}^{7} H_r(zW_8^k)H_c(z^{-1}W_8^{-k})S_{xx}(zW_8^k)$$

H_j(z): j^{th} element in row vector H(z)
Also the compensation vector

$$\underline{K} \;=\; 2\{2\,A\,P\,A + Q\}^{-1}A\,T \qquad (9)$$

where

$$P = \frac{1}{2\pi j}\oint B(z)\mathrm{diag}\left\{1,1,2,4\right\}P'(z)\mathrm{diag}\left\{1,1,2,4\right\} \cdot B(z^{-1})z^{-1}dz$$

$$Q = \frac{1}{2\pi j}\oint B(z)\mathrm{diag}\left\{2\sigma^2_{r_0}, 2\sigma^2_{r_1}, 4\sigma^2_{r_2}, 8\sigma^2_{r_3}\right\} \cdot B(z^{-1})z^{-1}dz$$

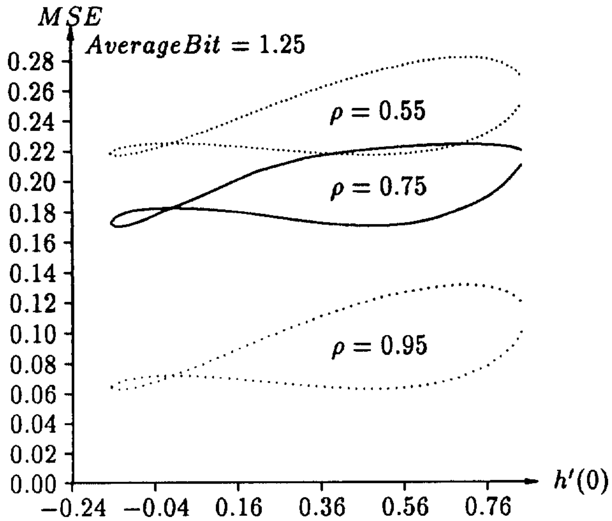

Fig.3

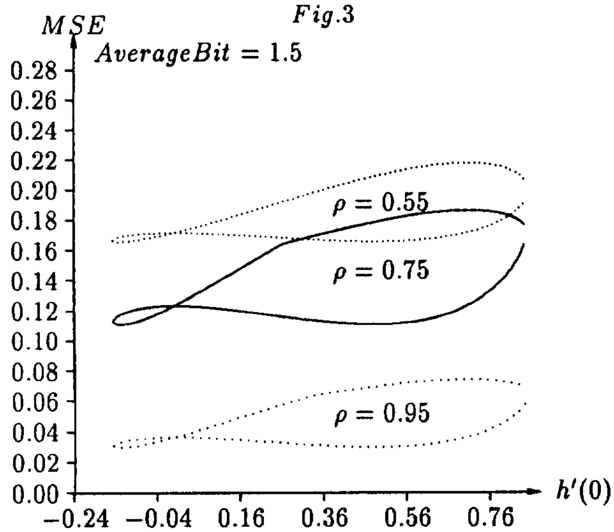

Fig.4

$$T = \frac{1}{2\pi j} \oint B(z) \mathrm{diag}\{1,1,2,4\} S_{xx}(z) \cdot z^{21} \begin{bmatrix} A_0(z) \\ A_1(z) \\ A_2(z) \\ A_3(z) \end{bmatrix} z^{-1} dz$$

$$B(z) = \mathrm{diag}\{B_0(z), B_1(z), B_2(z), B_3(z)\}$$

$$P'(z) = \begin{bmatrix} P''(0,0,8) & P''(0,1,8) & P''(0,2,4) & P''(0,3,2) \\ P''(1,0,8) & P''(1,1,8) & P''(1,2,4) & P''(1,3,2) \\ P''(2,0,4) & P''(2,1,4) & P''(2,2,4) & P''(2,3,2) \\ P''(3,0,2) & P''(3,1,2) & P''(3,2,2) & P''(3,3,2) \end{bmatrix}$$

where

$$P''(r,c,t) \triangleq \frac{1}{8} \sum_{k=0}^{t-1} A_r(zW_t^k) A_c(z^{-1}W_t^{-k}) S_{xx}(zW_t^k)$$

4 Design example

We assume identical 4 tap paraunitary filters in each stage and impose the requirement that the low pass filter has zero gain at $\omega = \pi$. This leaves only one unconstrained filter coefficient. We do an exhaustive search among all possible bit allocations and select the bit allocation and filter coefficient with the smallest MSE as demonstrated in Fig. 3 and Fig. 4. The average bit rate is constrained by

$$R_0 + R_1 + 2R_2 + 4R_3 = 8R_{ave}$$

Finally optimal filter coefficient is obtained as in table 1. It is nothing but binomial filter coefficient [1]. Table 2 shows optimal bit allocation corresponding to R_{ave}, correlation coefficient for AR(1) source. Compensation vector is the same as [4]. Simulation results(MSE_{sim}) by 20,000 samples are also shown.

optimal filter coefficients			
$h'(0)$	$h'(1)$	$h'(2)$	$h'(3)$
0.4829628	0.8365163	0.2241440	-0.1294096

table1

ρ	R_{ave}	R_0	R_1	R_2	R_3	MSE	MSE_{sim}
0.95	1.25	3	1	1	1	0.0629793	0.0618888
	1.5	4	2	1	1	0.0297709	0.0301811
0.75	1.25	3	1	1	1	0.1704207	0.1701666
	1.5	3	3	1	1	0.1106226	0.1109793
0.55	1.25	2	2	1	1	0.2171357	0.2158834
	1.5	2	2	2	1	0.1654545	0.1630787

table2

References

[1] Ali N. Akansu and R. A. Haddad, *Multiresolution Signal Decomposition: transforms subbands wavelets.* Academic Press, 1992.

[2] P. Hoang and P P. Vaidyanathan, "Non-Uniform Multirate Filter Banks: Theory and Design", *IEEE ISCAS*, 1989.

[3] N.S.Jayant and P.Noll, *Digital Coding of Waveforms.* Englewood Cliffs,NJ:Prentice-Hall,1984.

[4] Kyusik Park and R. A. Haddad, "Optimum subband filter bank design and compensation in presence of quantizer," *Proc. 27th Asilomar Conf. on Sign. Syst. and Comp.*, Pacific CA, Nov. 1993.

[5] A.Papoulis, *Probability, Random Variables, and Stochastic Processes.* 3rd Edition, pp.373-376,McGraw-Hill,NY,1991.

[6] Necdet Uzun, "Cyclostationary Modeling, Analysis and Optimal Compensation of Quantization Effects in Subband Codecs", Ph.D. dissertation, Polytecnic Univ., Brooklyn,NY,June. 1993.

[7] P.H.Westerink,J.Biemond,and D.E.Boekee, "Scalar Quantization Error Analysis for Image Subband Coding Using QMF's", *IEEE Trans. on Signal Processing*,vol.40,no.2, pp.421-428,Feb.1992.

[8] J.W.Woods and T.Naveen "A Filter Based Bit Allocation Scheme for Subband Compression of HDTV", *IEEE Trans. on Image Processing*,vol.1,no.3, pp.436-440,July 1992.

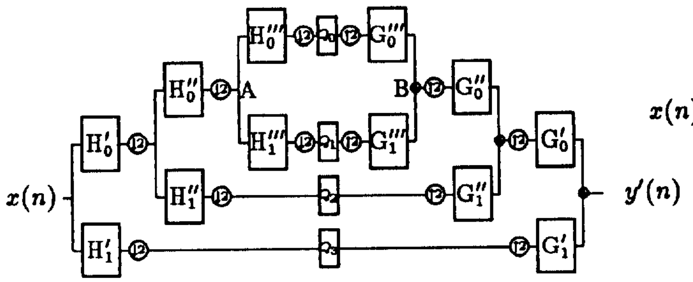

Fig.5

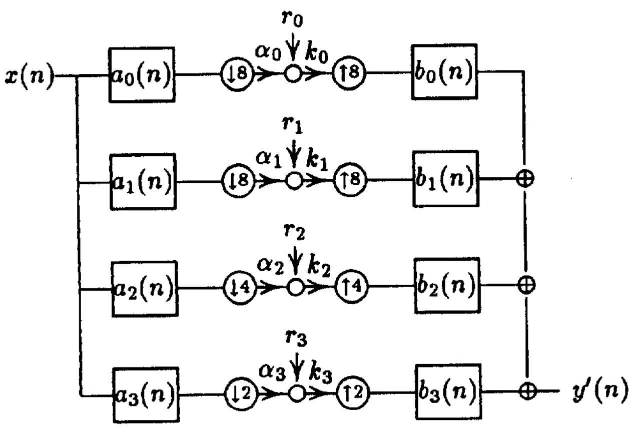

Fig.6

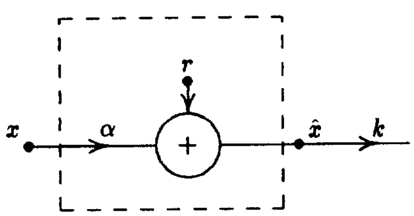

Fig.7

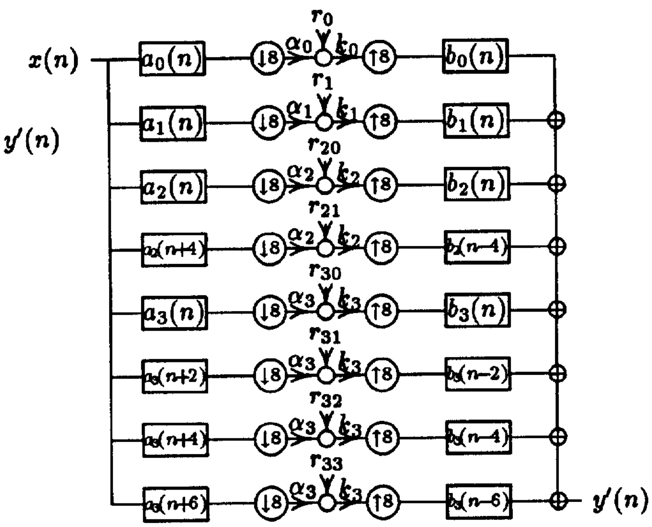

Fig.8

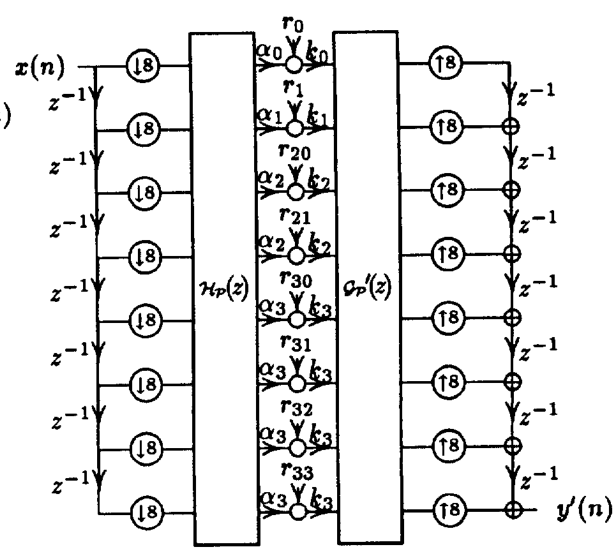

Fig.9